

Fluctuation-driven capacity distribution in complex networks

Dong-Hee Kim and Adilson E. Motter

Department of Physics and Astronomy and Northwestern Institute on Complex Systems (NICO), Northwestern University, Evanston, IL 60208, USA

E-mail: dongheekim@northwestern.edu and motter@northwestern.edu

Abstract. Maximizing robustness and minimizing cost are common objectives in the design of infrastructure networks. However, most infrastructure networks evolve and operate in a highly decentralized fashion, which may significantly impact the allocation of resources across the system. Here we investigate this question by focusing on the relation between capacity and load in different types of real-world communication and transportation networks. We find strong empirical evidence that the actual capacity of the network elements tends to be similar to the maximum available capacity if the cost is not strongly constraining. As more weight is given to the cost, however, the capacity approaches the load *nonlinearly*. In particular, all systems analyzed show larger unoccupied portion of the capacities on network elements subjected to smaller loads, which is in sharp contrast with the assumptions involved in (linear) models proposed in previous theoretical studies. We describe the observed behavior of the capacity-load relation as a function of the relative importance of the cost by using a model that optimizes capacities to cope with network traffic fluctuations. These results suggest that infrastructure systems have evolved under pressure to minimize local failures but not necessarily global failures that can be caused by the spread of local damage through cascading processes.

PACS numbers: 89.75.Fb, 89.75.Hd, 05.65.+b, 02.50.-r

Keywords: disordered systems, statistical physics, self-organization, complex networks

Published in: *New J. Phys.* 10, 053022 (2008)

1. Introduction

Various problems of immediate social and economical interest, ranging from the likelihood of power outages [1] and Internet congestion [2] to the affordability of public transportation [3], are ultimately constrained by the extent to which the assignment of capabilities matches supply and demand under realistic conditions. Continuous effort has been made to enhance the performance and limit the cost of individual system components, such as power transmission lines, computer routers and roads, with outcomes impacting the efficiency of virtually all infrastructure systems. Yet, the relation between the *large-scale* allocation and actual usage of resources in distributed infrastructure systems remains essentially unexplored and unexplained. For example, in a system as costly and up-to-date as the Internet router network, we find that on average more than 94% of the available bandwidth remains unused, which is comparable to the usage of data networks reported in previous studies [4].

We investigate this problem by focusing on the relationship between *capacity* and *load*. We first note that the activity of many infrastructure systems can be modeled as a network transport process. For example, website browsing and e-mail communication are based on packet transport through the Internet, movement of people and goods is heavily based on road, rail, and air transportation networks, while the provision of public utility services depends on the transport of energy, water and gas carried by power grids and other supply networks. In these examples, the transport of packets, passengers, and physical quantities creates traffic loads that must be handled by nodes and links of the underlying networks. In order to provide stable functioning, the capacities of nodes and links have to be large enough to handle the loads under variable conditions. On the other hand, the capacities are limited by cost and availability of resources, which increases the probability of failures if loads increase. Proper allocation of capacities is thus a basic requirement for the robust and efficient operation of infrastructure networks.

The recent realization that numerous systems can be modeled within the common framework of complex networks [5, 6] has stimulated many theoretical studies on structural resilience [7, 8, 9, 10, 11, 12] and congestion problems [13, 14, 15, 16, 17] as well as cascading failure [18, 19, 20, 21, 22, 23, 24, 25, 26, 27] and cascade control analysis [28, 29, 30, 31, 32, 33, 34]. Studies of air transportation networks [35, 36], in particular, have shown that the strengths of the network connections may follow a pattern partially determined by the network topology [37, 38]. However, despite much advance, the determination of the capacity and load characteristics of real networks is a question that goes beyond previous complex network research.

Here we study this question from the perspective of a decentralized optimization between *robustness* and *cost*. We analyze four types of infrastructure networks, the air transportation, highway, power-grid and Internet router system. We find empirically that the capacity-load relation is mainly determined by the relative importance given to the cost and exhibits an unanticipated nonlinear behavior, which, as shown schematically in Figure 1, is very different from the constant [20, 21], random [18, 27], and

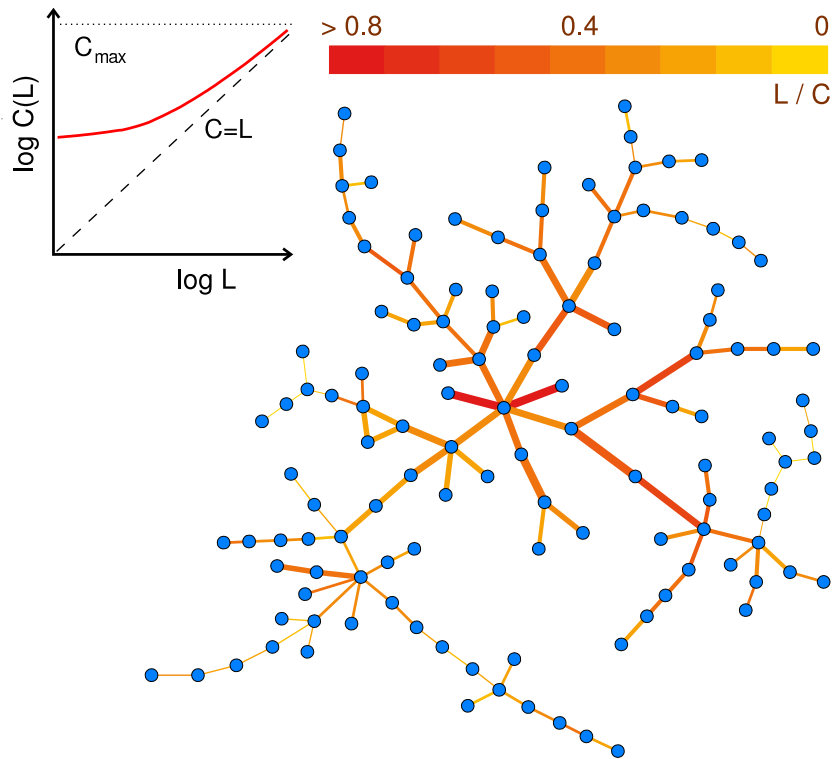


Figure 1. Capacity allocation pattern in a sampled part of the US power-grid network. The color and width of the links indicate the load and capacity of the transmission lines, respectively. The top left panel indicates the typical overall capacity-load relation observed in real infrastructure networks, where components with larger capacity have larger load-to-capacity ratio.

linear [19, 22, 24, 25, 26, 30] assignments of capacities considered in previous models (see also [31, 32, 33]). We study this nonlinearity using the concept of *unoccupied capacity*, which we defined as the difference between the capacity and the time-averaged load. It follows that the percentage of unoccupied capacity is smaller for network elements with larger capacities.

We demonstrate the observed behavior using a traffic model devised to minimize the probability of overloads in a scenario of fluctuating traffic and limited availability of resources. This model accommodates the interpretation that the empirical distributions follow from a decentralized evolution in which capacities and loads are (re)allocated in response to network stress caused by increasing load demand. In the US power grid, for example, the load demand increases by 2% per year and detectable blackouts occur on an average of one every 13 days [39, 40]. Despite being driven by a decentralized process, the long term accumulation of local changes can give rise to an organized pattern in the capacity-load relation, suggesting similarities between network evolution and other self-organized phenomena [39, 40, 41]. In particular, our model shows that the reduction of the unoccupied capacity in high-capacity elements is mainly a consequence of the reduction of the traffic fluctuations for higher loads, but it also shows that the probability

of overloads can be larger on elements with *larger* capacities. These results should enable researchers to build models to gain insights into the evolution of decentralized systems and, in particular, to evaluate the impact of disturbances in large communication and transportation networks.

2. Empirical Data and Capacity-Load Characteristics

We investigate the properties of load and capacity distributions in four different types of real-world infrastructure networks: power-grid network, highway network, Internet router network, and air transportation networks. In each of these systems, the load and capacity are defined considering the type of traffic on the network, namely, electric power in the power grid, traffic of vehicles in the highway network, packet flow in the Internet, and passengers and aircraft in the air transportation networks. The load represents an averaged quantity over a period of time in all the networks considered. Figure 2 shows the relationship between the load and capacity for the network elements in the respective systems. In the analysis of the real data, we find that the capacity-load relation depends on the specific network, but the pattern of this dependence can be understood as the result of a trade-off between the cost of the capacities and the robustness of the network. In the following, we discuss in detail the datasets examined and the empirical capacity-load characteristics.

2.1. Air Transportation Networks

2.1.1. Airway Network. We analyze the aviation data available at the Bureau of Transportation Statistics database (<http://www.bts.gov>), which contains the seat occupation data of US and foreign aircraft operating between 1449 US and foreign airports in the year 2005. Flights with both origin and destination outside the US are not included in the database. The load L and the capacity C of an airway connecting two airports are defined as the total number of occupied and available seats of all flights connecting the airports, respectively. Figure 2(a) shows that the airway network has a very efficient capacity distribution. While there are data points with the capacity larger than the load, the capacity-load relation is very close to the line of maximum efficiency $C(L) = L$. This efficiency is likely to be related to the high costs of air transportation, which create strong incentives for the airline companies to operate with a high occupancy factor.

2.1.2. Airport Network. We also examine a different dataset obtained from the International Air Transportation Association (IATA) [42], which reflects the operation and physical capacity of 90 major international airports in 2002. In the airway network considered above, the load and the capacity are defined for *links* (airways) as the total occupied and total available number of seats in flights connecting two airports, respectively. In contrast, for this dataset, we define the load and capacity

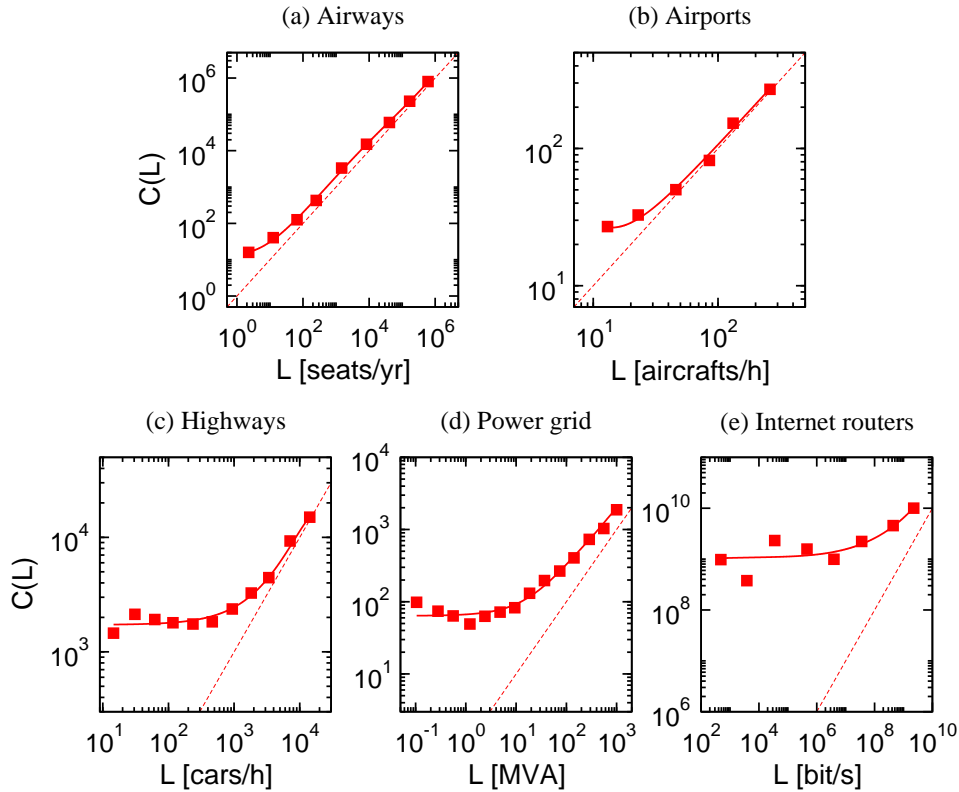


Figure 2. Capacity-load relation of real infrastructure networks. (a) Total number of occupied (L) versus available seats (C) in aircraft departing from and arriving at 1449 US and international airports in 2005. (b) Peak-hour aircraft movements (L) and nominal peak-hour capacity (C) of 90 international airports in 2002. (c) Design hourly volume (L) versus estimated capacity (C) of 1559 Colorado highway segments in 2005. (d) Apparent power (L) versus maximum apparent power (C) of 5855 transmission lines in the power grid of Texas in the summer peak of 2000. (e) Monthly averaged traffic (L) versus bandwidth (C) of the 721 router interfaces of the ABILENE backbone, MIT and Princeton University networks in June 2006. The filled boxes with curve fits indicate the averaged capacity-load relation $C(L)$ calculated in a logarithmic scale. The line of maximum efficiency $C = L$ (dashed line) is shown for comparison with the data.

for *nodes* (airports) as the peak-hour aircraft movements (arrivals + departures) and corresponding capacity declared by each airport. We call this network the *airport* network to distinguish from the *airway* network. Figure 2(b) shows that the capacity-load relation of the airport network is close to the line $C(L) = L$, indicating that very large airports tend to operate close to full capacity ‡.

‡ Because the *declared* capacity is not necessarily a sharp limit, some airports can be found to operate above the capacity in Figure 2(b).

2.2. Highway Network

We examine the traffic data of the state of Colorado in the year 2005 for 1559 highway segments available at the Colorado Department of Transportation database (<http://www.dot.state.co.us>). For each segment, we define the subjected load L as the design hourly volume (the 30th highest annual hourly traffic volume) in units of the number of cars per hour, which is regarded as the typical peak hour traffic volume for operational and design purposes [43]. Since the capacity itself is not available in the database, C is estimated from the volume-to-capacity ratio ($\sim L/C$) and the design hourly volume L . Figure 2(c) indicates that the capacity-load relation of the highway network is different from that of the airway network in the region of small loads. While the capacity is close to the load for the highway segments with large loads, there are many secondary segments with capacities much larger than their loads. This indicates that, as compared to the air transportation network, efficiency has a lower priority in the highway network. In this system, the segments with $C \gg L$ may provide an alternative route for congested traffic and attenuate jamming in peak hours. However, the behavior $C \sim L$ in the large L region suggests that the cost is also an important limiting factor in the construction and maintenance of the highway system.

2.3. Power-Grid Network

We consider the power-grid network of the Electric Reliability Council of Texas (<http://www.ercot.com>) and analyze the maximum apparent power (S_{\max}), the real power (P) and the reactive power (Q) measured at the summer peak of the year 2000 for 5885 transmission lines. We define the load and the capacity of a transmission line as the apparent power ($L \equiv \sqrt{P^2 + Q^2}$) and its maximum allowed value ($C \equiv S_{\max}$) in units of MVA, respectively. Figure 2(d) shows a pattern similar to the one observed in the highway network: there exists an abundance of transmission lines with the capacities much larger than the loads. In a power grid, the robustness may be even more important than in a highway network because once a failure cascades, such as in the August 14, 2003 North America blackout, it can cause losses in a very large scale. Compared to the highway network, the power grid has larger unoccupied capacities for the heavily loaded components of the network, a feature that is useful in this case for the dispatch of power generation to adjust to specific market, weather, and demand conditions.

2.4. Internet Router Network

We analyze the average packet traffic data in June 2006 monitored by the Multi Router Traffic Grapher (<http://oss.oetiker.ch/mrtg/>) in the 721 routers of the ABILENE backbone, MIT, and Princeton University networks. We define the load L and the capacity C of a router respectively as the monthly average of occupied and available bandwidth of the network interface of the router in units of bps (bit/s). Figure 2(e) shows a weaker dependence of the capacity on the load than those found for the other

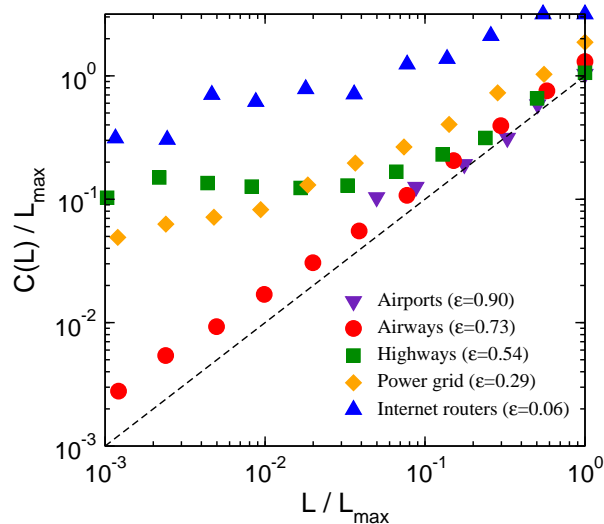


Figure 3. Averaged capacity-load relation of the air transportation networks, highway network, power-grid network, and Internet router network along with the corresponding efficiency coefficient ε . The data for the load are log-binned to obtain the averaged relation $C(L)$. For a comparison between networks having different ranges of capacity and load, the data are normalized by the maximum load value L_{\max} . Data points with very small load ($L/L_{\max} < 10^{-3}$) do not affect the tendency and are not shown.

networks, which a property partially explained by the discreteness of the capacities in the Internet router network. There are, indeed, only few classes of router interfaces commercially available, with bandwidths of 10 Mbps, 100 Mbps, 1 Gbps, 10 Gbps, and so on. Routers in the same group, such as the same university or the same backbone network, tend to be simultaneously upgraded to an upper class of capacities, regardless of their actual individual loads. The substantial upgrades required by the fast growing bandwidth demand contribute to the observed large margin of unoccupied capacities. Thus, compared to the other networks, one can argue that in the Internet router system robustness is prioritized over cost.

2.5. Efficiency Coefficient

The analysis above provides evidence that the capacity allocation pattern can be traced back to the importance of the cost in the construction and maintenance of the system. For a quantitative explanation, we introduce the *efficiency coefficient* ε of the network, which we define as the ratio between the total load $\sum_i L_i$ and total capacity $\sum_i C_i$ of the system:

$$\varepsilon = \frac{\sum_i L_i}{\sum_i C_i}. \quad (1)$$

This quantity serves as a measure of the importance of the cost versus robustness §. As the cost becomes more important, the capacity is expected to be set closer to the load to prevent overallocation of resources, which increases ε .

This tendency is confirmed in Figure 3, where we show how the averaged capacity-load relation $C(L)$ depends on the efficiency coefficient ε for all networks analyzed. The efficiency coefficient is $\varepsilon = 0.73$ (airways) and $\varepsilon = 0.90$ (airports) for the air transportation networks, 0.54 for the highway network, 0.29 for the power-grid network, and 0.06 for the Internet router network. The extremely high efficiency coefficient of the airport network may be partially related to the fact that this database refers to major airports only. However, as illustrated in the case of the power-grid and highway network, which have different trends for small L , the overall efficiency coefficient can be dominantly determined by the most loaded elements in the network (note the logarithmic scale in Figure 3) ||.

3. Capacity Optimization and Traffic Fluctuation Model

Having identified the capacity-load characteristics of real-world networks, we now study the empirical findings using a theoretical model based on optimizing the capacity and the cost at the level of individual nodes or links. We define a simple objective function F_i for node (or link) i as

$$F_i = (1 - w)R_i(C_i) + wS_i(C_i), \quad (2)$$

where $R_i(C_i)$ and $S_i(C_i)$ are the robustness and the cost function, respectively, and the weight factor $w \in [0, 1]$ represents the importance of the cost. If we choose the robustness R_i (cost S_i) to be a decreasing (increasing) function of C_i , the minimization of F_i will lead to an optimized capacity C_i for node i subjected to the time-averaged load L_i , which defines a capacity-load relation $C(L)$.

In order to determine the robustness function, it is important to identify the main source of perturbation affecting the system. While the information about the entire network is quite limited in general, the local time-variations of load provide valuable information about the vulnerability of the individual network components. Here we consider the fluctuation of traffic over time as the sole perturbation that can causes accidental failure or malfunctioning due to overloading. Traffic fluctuation is a fundamental and ubiquitous property of the traffic dynamics which has been studied for a wide range of real networks [45, 46]. Recent studies have reported that in Internet routers, microchips, rivers and highways, the average traffic load L and the standard

§ Note that the efficiency coefficient accounts for the usage of the available capacities rather than the efficiency of the routing algorithm [44].

|| To further examine the contribution of large loads and capacities, we also considered a modified definition of the efficiency coefficient, $\epsilon' = \sum \log(L_i) / \sum \log(C_i)$, which leads to $\epsilon' = 0.97$ (airports), 0.92 (airways), 0.84 (highways), 0.67 (power grid) and 0.57 (Internet routers). This indicates that, while the value of the efficiency coefficient itself would change, the tendency across the systems remains the same even if less emphasis is given to the elements with large L and C .

deviation of the load σ are related through the scaling $\sigma \sim L^\alpha$ with $\alpha = 0.5 - 1.0$ [46, 47, 48]. This further indicates that the capacity designed to tolerate traffic variability can be expressed in terms of the average load.

We model the traffic fluctuations using a simple transport process in which a certain amount $x_{jk}(t)$ of traffic is created at a source node j at time t and moves to a destination node k along a predetermined path. This process includes as a special case the directed flow model introduced in a previous study [46], where random pairs of source and destination nodes are selected for the creation of traffic at each time step and the traffic moves along the shortest path. Here we consider a more general yet mathematically treatable model that is less dependent on the details of the network structure and routing rules. A simple microscopic description of our model has been anticipated in [49].

In our model, we define the load $l_i(t)$ as the amount of traffic processed per unit time at node i measured during a time window δt . Formally, we can write the load $l_i(t)$ as

$$l_i(t) = \frac{1}{\delta t} \int_t^{t+\delta t} dt' \int_{-\infty}^{t'} dt'' \sum_{j,k} x_{jk}(t'') \Phi_{jk}(t''; i, t'), \quad (3)$$

where $\Phi_{jk}(t''; i, t')$ is a propagator of the traffic towards node k starting from node j at time t'' and passing through node i at time t' . For transport through predetermined paths, $\Phi_{jk}(t''; i, t')$ can be rewritten using the travel time $t_{jk}^{(i)}$ elapsed to reach node i as $z_{jk}^{(i)} \delta(t'' + t_{jk}^{(i)} - t')$, where $z_{jk}^{(i)}$ is 1 if the traffic from j to k passes through i and 0 otherwise. Then, $l_i(t)$ can be simplified as

$$l_i(t) = \sum_{j,k} z_{jk}^{(i)} r_{jk}^{(i)}(t) \equiv \sum_{j,k} z_{jk}^{(i)} \left[\frac{1}{\delta t} \int_t^{t+\delta t} dt' x_{jk}(t' - t_{jk}^{(i)}) \right]. \quad (4)$$

To identify the stochastic characteristics of $l_i(t)$, a reference we use for capacity determination, the measurement time δt can be chosen to be of the order of the autocorrelation time of the load fluctuation $\sum_{j,k} z_{jk}^{(i)} x_{jk}(t - t_{jk}^{(i)})$. Then, we can obtain the distribution of loads $P_i(l_i)$ for a large number of δt intervals and thereby the overloading probability ξ_i , which can be derived as

$$\xi_i(C_i) = \text{Prob}[l_i > C_i] = \int_{C_i}^{\infty} P_i(l_i) dl_i \quad (5)$$

for given capacity C_i such that $L_i \leq C_i \leq C_{\max}$, where $L_i = \int l_i P_i(l_i) dl_i$. We assume that the capacity C_i is physically upper-bounded by the maximum value C_{\max} and is lower-bounded by the line of maximum efficiency $C = L$.

We choose the overloading probability as the robustness function so that $R_i(C_i) \equiv \xi_i(C_i)$, where a smaller overloading probability represents a higher robustness in a probabilistic sense. The cost function is defined for concreteness as a linear function of the capacity, $S_i(C_i) \equiv C_i/C_{\max}$. Therefore, we can rewrite the objective function explicitly as

$$F_i = (1 - w)\xi_i(C_i) + w \frac{C_i}{C_{\max}}, \quad (6)$$

where $L_i \leq C_i \leq C_{\max}$. The optimized distribution of capacities can now be calculated by minimizing this objective function.

In order to explicitly calculate the capacity-load relation within this optimization model, we consider both uncorrelated and synchronized traffic fluctuations under the condition that every traffic creation event shares identical statistical properties. In the case of the uncorrelated fluctuations, a traffic creation event at a node is statistically uncorrelated with those at the other nodes. In the case of the synchronized fluctuations, on the other hand, we assume that every node creates the same amount of traffic simultaneously. It is worthwhile considering both types of fluctuations in view of the recent empirical evidence [47] that random internal fluctuations can be strongly modulated by external driving forces. In the Internet backbone, for example, it has been observed that the traffic dynamics is well characterized by a Poisson process for millisecond time scales, while long-range correlations appear for longer time scales [50].

3.1. Uncorrelated Fluctuations

We consider uncorrelated fluctuations in which the amount of traffic $r_{jk}^{(i)}(t)$ created at the source node j and moving to the destination node k is completely uncorrelated with the traffic between different source-destination node pairs. In this regime, the quantity $r_{jk}^{(i)}(t)$ can be regarded as an independent identically distributed random variable r following a probability distribution $p(r)$. Therefore, assuming that $p(r)$ has finite moments, including average \bar{r} and variance s^2 , we apply the Central Limit Theorem [51] to calculate the distribution of loads. This leads to a Gaussian distribution of loads

$$P_i(l_i) \simeq \frac{1}{\sigma_i \sqrt{2\pi}} \exp \left[-\frac{(l_i - L_i)^2}{2\sigma_i^2} \right], \quad (7)$$

with the average $L_i = \bar{r}z_i \equiv \bar{r} \sum_{j,k} z_{jk}^{(i)}$ and the variance $\sigma_i^2 = s^2 z_i$. Note that the relation $\sigma_i \sim L_i^{1/2}$, a corollary of (7), is in agreement with the results of previous studies [46, 47, 48].

Using (7), we can obtain the solution of the optimized capacity-load relation $C(L)$ by minimizing F in (6). The resulting capacity-load relation is expressed as $C(L) = \min\{C'(L), C_{\max}\}$ with

$$C'(L) = \begin{cases} L + gL^{\frac{1}{2}} \sqrt{\log \Omega(L)} & \text{if } L < L_w, \\ L & \text{if } L > L_w, \end{cases} \quad (8)$$

where

$$\Omega(L) \equiv \frac{1}{g\sqrt{\pi}} \frac{1-w}{w} \frac{C_{\max}}{L^{1/2}}, \quad (9)$$

parameter g denotes $\sqrt{2s^2/\bar{r}}$, and L_w satisfies $\Omega(L_w) = 1$.

3.2. Synchronized Fluctuations

To implement synchronized fluctuations within our model, we assume the following properties of the traffic variables. First, while the uncorrelated fluctuations occur in

a short time scale, the modulation that we attempt to describe by the synchronized fluctuations occur in a much longer time scale [47, 48]. Such a synchronization can be generally triggered by exogenous factors, such as weather and seasonal conditions, or collective behavior. Second, we assume that the travel time $t_{jk}^{(i)}$ is much shorter than the time scale of the modulation. Then, neglecting the travel time $t_{jk}^{(i)}$ and using that the synchronized traffic creation $x_{jk}(t)$ can be represented by a single function $x(t)$, we can set $r_{jk}^{(i)}(t) \equiv r(t)$ to write the load as $l_i(t) = r(t)z_i$.

Assuming statistical independence of $r(t)$'s in different modulation periods, we consider the stochastic characteristics of the peak value of $r(t)$ defined in each modulation period as a reference for capacity determination. Given the distribution of the peak values $p(r)$ in many different modulation periods, we can write the overloading probability ξ_i for a given capacity C_i as

$$\xi_i(C_i) = \int_{C_i}^{\infty} P(l_i) dl_i = \int_{\bar{r}C_i/L_i}^{\infty} p(r) dr, \quad (10)$$

where the average load is $L_i = \bar{r}z_i$ and $\bar{r} = \int r p(r) dr$.

By minimizing the objective function F in (6), the optimized capacity is obtained as $C = \min\{C'(L), C_{\max}\}$ with

$$C'(L) = \begin{cases} \frac{L}{\bar{r}} q\left(\frac{w}{1-w} \frac{L}{\bar{r}C_{\max}}\right) & \text{if } L < L_w, \\ L & \text{if } L > L_w, \end{cases} \quad (11)$$

where $L_w \equiv \bar{r}C_{\max} \frac{1-w}{w} \max_r p(r)$ and $q(y) = r$ is obtained by inverting $y = p(r)$. For $p(r)$ having a single maximum, while two solutions of r are generally possible in the equation $y = p(r)$, we conventionally select $q(y)$ with the larger value of r , which gives the larger capacity.

The distribution $p(r)$ is the final ingredient for the explicit calculation of $C(L)$ in the synchronized fluctuation regime. Because we have defined r as the maximum value of many traffic creation events, the distribution of maxima in the extreme value statistics can be used as an input for $p(r)$ in the model. Here we numerically calculate $C(L)$ for the Gumbel distribution $p_g(r)$ and the Fréchet distribution $p_f(r)$, referred to as the first and second asymptotes in the extreme value statistics literature [52], which are written as

$$p_g(r) = \frac{1}{\beta} \exp\left[-\frac{r-\mu}{\beta} - e^{-\frac{r-\mu}{\beta}}\right], \quad (12)$$

$$p_f(r) = \frac{\gamma}{\alpha^{-\gamma}} r^{-\gamma-1} \exp\left[-\left(\frac{r}{\alpha}\right)^{-\gamma}\right], \quad (13)$$

where all parameters are positive. These extreme value distributions cover two types of unbounded initial distributions, the exponential type for p_g and the power-law type for p_f . The third asymptote is for strictly bounded initial distributions and gives similar results as the bound of the created traffic becomes large.

Figure 4 shows the numerically calculated capacity-load relation $C(L)$ for uncorrelated and synchronized fluctuations. In both regimes we find that the allocation of capacities exhibits characteristics in common with the empirical data. In particular,

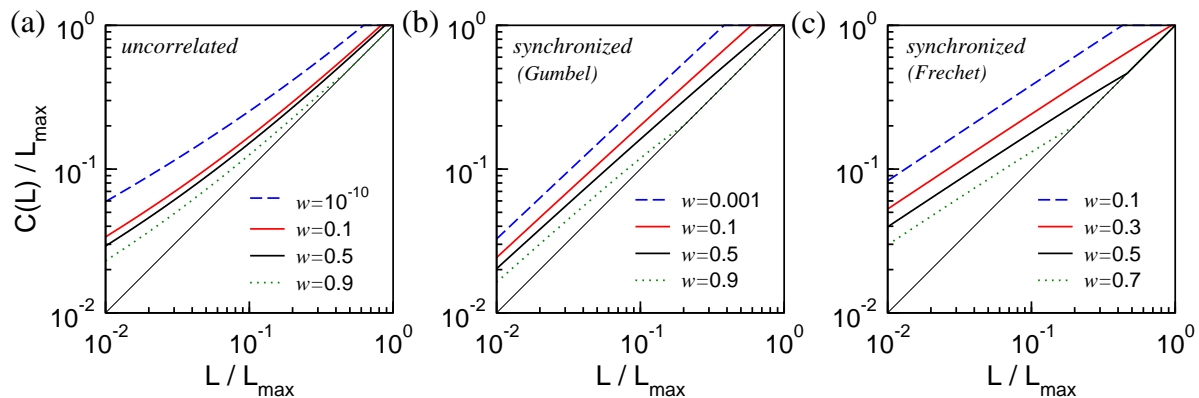


Figure 4. Capacity-load relation predicted by the optimization model for different values of the weight w given to the cost: (a) uncorrelated fluctuation regime and (b-c) synchronized fluctuation regimes. The model parameter $g = 3$ is used for the uncorrelated regime. The extreme value distributions are assumed to be (b) the Gumbel distribution with parameters $(\mu, \beta) = (100, 20)$ and (c) the Fréchet distribution with $(\alpha, \gamma) = (1, 2)$. The capacity and load are normalized by the predefined maximum value $C_{\max} = L_{\max} = 10^3$.

as the weight factor w decreases (reducing the importance of the cost), in all cases the curve $C(L)$ recedes from the line $C = L$ and moves up towards the line $C = C_{\max}$. More important, the calculated $C(L)$ shows the common trend that a larger relative deviation from the linear line $C = L$, representing a larger unoccupied portion of the capacity, is found in the region of smaller L . We note that our model, and hence the conclusions we draw from it, are determined by general statistical properties of the traffic and do not depend on the details of the network structure and dynamics. This generality represents an advantage over previous models based on betweenness centrality because, as shown in Appendix A, the latter is only weakly correlated with the actual flow in the networks and cannot provide information about $C(L)$.

The traffic fluctuations considered in our model reflect a realistic feature of infrastructure networks. However, it remains an open problem to develop a fully realistic model. One possible direction for future research is to consider intermediate regimes that incorporate both uncorrelated and synchronized fluctuations. This is relevant for situations in which a synchronized perturbation occurs together with uncorrelated background fluctuations. Another direction concerns the incorporation of network-structure dependence of traffic control and capacity determination. In the case of the Internet router network, for example, previous works have shown that the capacity and degree are *negatively* correlated [53], suggesting a potential relation between the network topology and the exceptionally large nonlinearity in the capacity-load relation of Figure 2(e). In addition, it is valid to consider the impact of the apparent lower bound in the capacities [54], which may further contribute to the observed nonlinearity.

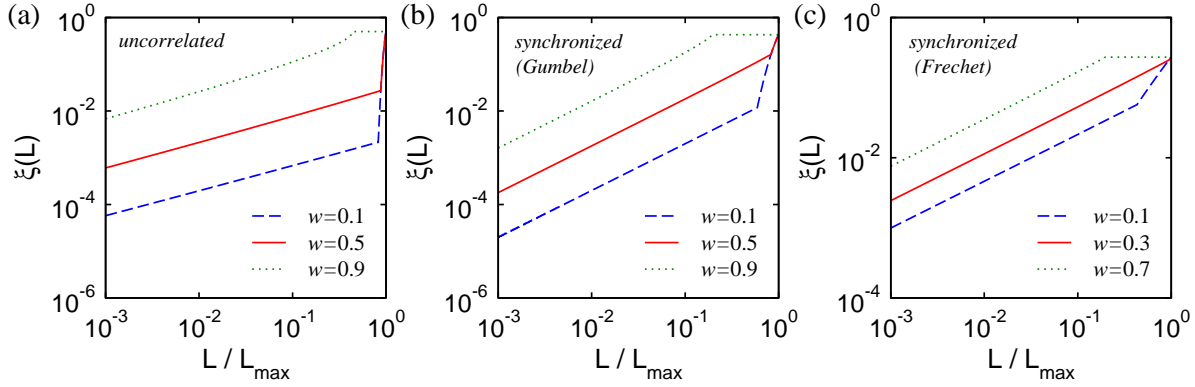


Figure 5. Overloading probability for the optimized capacities in (a) the uncorrelated and (b-c) synchronized fluctuation regimes. The unspecified parameters are the same as in Figure 4.

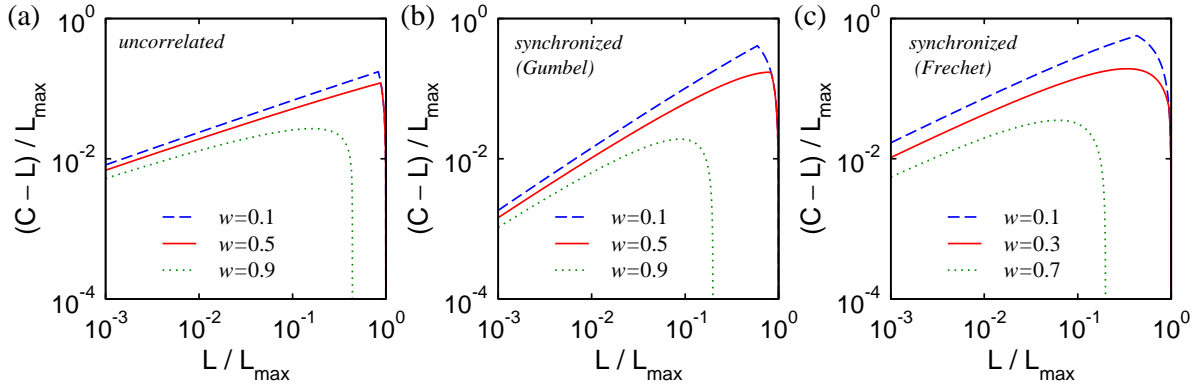


Figure 6. Unoccupied capacity $(C - L)$ for the optimized capacities in (a) the uncorrelated and (b-c) synchronized fluctuation regimes. The parameters are the same as in Figure 5.

4. Unoccupied Capacity and Overloading Probability

Our empirical results are in sharp contrast with the linear capacity-load relation hypothesized in previous work, and our model shows that the apparently universal nonlinear behavior is a consequence of fluctuations in the traffic load. Because larger loads tend to result from a larger number of traffic events, the relative size of the fluctuations tend to decrease as the load increases; considering that the unoccupied capacity is mainly determined by the perturbations caused by traffic fluctuations, this explains why the unoccupied portion of the capacity is observed to be smaller in network elements with larger loads and capacities. From this perspective, the observed decrease in the percentage of unoccupied capacity is a consequence of the law of large numbers.

However, the same analysis also reveals two surprising elements. First, the predicted overloading probability $\xi(L)$, calculated in (5) using (8) and (11), is larger for network elements subjected to larger loads, despite the fact that the capacities are also larger and the relative fluctuations are smaller (Figure 5). The explanation for this is that,

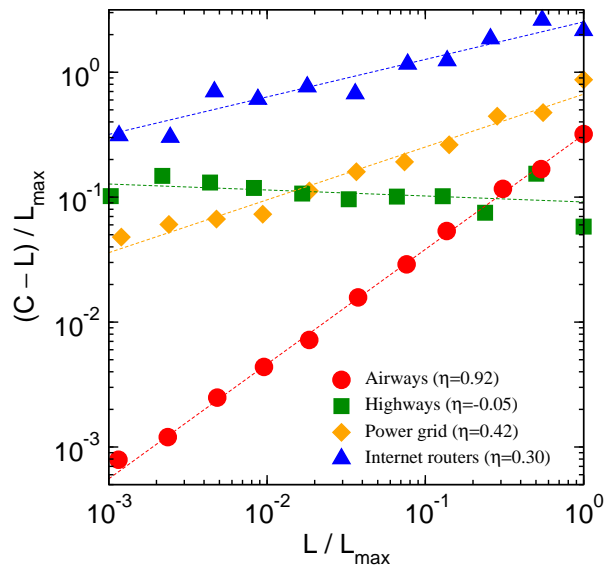


Figure 7. Unoccupied capacity ($C - L$) for the airway, highway, power-grid and Internet router network. The data are log-binned to obtain the average behavior of $C - L$ as a function of L . Curve fits $(C - L) \sim L^\eta$ are given for each network to compare with the theoretical model. For a comparison between networks having different ranges of capacity and load, the data are normalized by the maximum load L_{\max} .

although the relative size of the fluctuations decreases, their absolute size increases as the load increases. Therefore, the reduction in the unoccupied portion of the capacities as the load increases is not only a consequence of the decreasing fluctuations but also partially due to the optimization of capacities. For concreteness we have assumed that the cost is a linear function of the capacity, but similar or more pronounced behavior is predicted for superlinear cost functions (Appendix B). Second, the reduction in the unoccupied portion of the capacities is observed not only when the traffic events are statistically independent but also when the fluctuations are synchronized. For synchronized fluctuations, the sublinear behavior of $C(L)$ cannot be anticipated from (non-optimal) *egalitarian* solutions determined by an equal probability $\xi = \xi_c$ of overload for every node, since equal probabilities lead to a linear dependence $C \propto L$ in the capacity-load relation. Setting $\xi = \xi_c$ in (5), the capacity for the egalitarian solutions is derived as $C = L + g \operatorname{erf}^{-1}(1 - 2\xi_c)L^{1/2}$ in the uncorrelated regime, while the corresponding equation $\int_{\bar{r}C/L}^{\infty} p(r)dr = \xi_c$ leads to $C/L = \text{constant}$ in the synchronized regime. Therefore, while synchronized fluctuations are expected to consume more resources, the optimization of the capacities makes this less severe by allowing higher probability of overloads in components with larger loads. For uncorrelated fluctuations, the capacity has a sublinear term even for egalitarian solutions.

The real data corroborates the interpretation that the capacities are closer to optimal than to egalitarian solutions in three out of four systems analyzed ¶.

¶ The airport data is not considered here because it comprised few data points and leads to a statistically poor distribution for $C - L$.

Table 1. Unoccupied capacity. Exponents of a power-law curve fitting $C - L \sim L^\eta$ for egalitarian solutions and for solutions of the optimization model.

	optimized solutions	egalitarian solutions
uncorrelated fluctuations	$\eta < 0.5$	$\eta = 0.5$
synchronized fluctuations	$\eta < 1.0$	$\eta = 1.0$

follows from a comparison between the unoccupied capacity $C - L$ calculated from our optimization model (Figure 6) and the empirical unoccupied capacity (Figure 7). In the optimization model, $C - L$ increases sublinearly with L (except for the region of very large loads, where it decreases). This follows directly from (8) for uncorrelated fluctuations and (11) for synchronized fluctuations. The egalitarian capacity distribution also shows sublinear behavior for uncorrelated fluctuations, but the scaling exponent is different from the one obtained from the optimization model (Table 1). This difference can help determine the origin of the distributions in real networks. For the power-grid and Internet router network, $C - L$ grows sublinearly with L , consistently with the predicted optimal solutions for which the absolute value of the unoccupied capacity $C - L$ generally increases with L but it does so slower than $L^{1/2}$. For the highway network, $C - L$ is approximately constant in a wide range of the load. This interesting property of the highway network is an extreme example of the reduction in the portion of unoccupied capacity in the main elements of the system. For the airway network, $C - L$ is an approximately linear function of L . Although $p(r)$ in (11) cannot be easily determined within our model, this provides evidence that, in contrast with the other networks, the air transportation system is dominated by synchronized fluctuations and operates close to an egalitarian solution. Besides being strongly seasonal, the airway network is the only system in our dataset that allows for real-time capacity adjustment.

An important implication of the observed nonlinearity in the capacity-load relation is that infrastructure systems appear to have evolved under the pressure to minimize local failures rather than global failures. Previous work [28] has established that the incidence of large cascading failures can be reduced by removing low-loaded nodes, despite the fact that this causes the concurrent increase in the incidence of local failures. In the present model this would correspond to a higher probability of overloads $\xi(L)$ for small L , which is the *opposite* of the trend observed in this study. The apparent vulnerability to large-scale failures is consistent with the absence of global optimization in real-world infrastructure networks that evolve in a decentralized way. In the case of the power grid, for example, it has been proposed [40] that the evolution of the system is driven by the opposing forces of slow load increase and corresponding system upgrades. That is, the evolution is determined by a dynamic equilibrium near a point of overloading, which represents an optimized state balancing capacities and the probability of blackouts. It is likely that a similar self-organization mechanism is at work in infrastructure systems in general. While providing additional rationale for

the decentralized optimization incorporated in our model, this view emphasizes that in infrastructure systems local robustness is prioritized over global robustness.

5. Conclusions

We have presented a unified study of the large-scale pattern of resource allocation in diverse real-world infrastructure networks. Our empirical and theoretical analysis provides evidence that in all systems analyzed the determination of capacities results from a decentralized trade-off between cost and robustness. Our optimization model accounts for the perturbations introduced by traffic fluctuations and reveals that system-specific characteristics of the observed nonlinear behavior of the capacity-load relation are mainly determined by the weight given to the cost. It is interesting to note, however, that the capacity allocation is fairly independent of the details of the network structure and traffic dynamics, and it is well expressed as a function of the average load at individual network components. By describing both universal and system-specific characteristics, our analysis contributes to a unified understanding of self-organized patterns driven by decentralized evolution and operation, which is a problem that carries implications for the study of complex systems in general.

Acknowledgments

This work was supported by NSF under Grant No. DMS-0709212.

Appendix A. Capacity and load versus graph-theoretic centralities

In the study of complex networks, the importance of nodes and links is often estimated from graph-theoretic centralities [55] defined by the structure of the network. We have compared the empirical data with two widely used centralities, the degree and the betweenness centrality [55, 56, 57]:

$$k_i^{(out)} = \sum_j A_{ji}, \quad k_i^{(in)} = \sum_j A_{ij}, \quad b(g) = \sum_{i \neq j} \frac{h(i, j; g)}{h(i, j)},$$

where $k_i^{(out)}$ and $k_i^{(in)}$ denote the out-degree and in-degree of node i , respectively, and $b(g)$ denotes the betweenness centrality of a node or link represented by g . Here $A \equiv (A_{ij})$ is the adjacency matrix, $h(i, j; g)$ is the number of shortest paths from node i to node j passing through g , and $h(i, j)$ is the total number of shortest paths from i to j . The component A_{ij} of the adjacency matrix is defined as 1 if node i has an incoming link from node j and 0 otherwise.

Previous studies [57, 58] have found very broad distributions of node and link betweenness centralities in complex networks, which is also the case for the real-world networks we have considered here. However, as shown in Figure A1 for the power-grid and airway network, whose network topologies are available in our database,

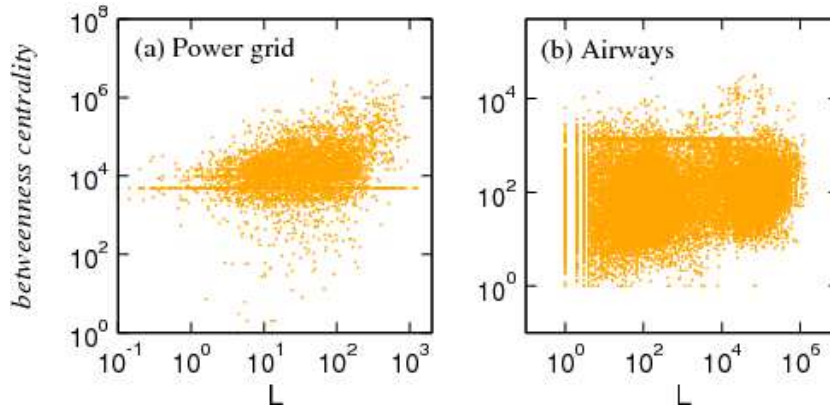


Figure A1. Comparison between empirical load and link-betweenness centrality. The scattered plots for (a) the power-grid and (b) airway network indicate that very small correlations exist between the empirical load and the link-betweenness centrality.

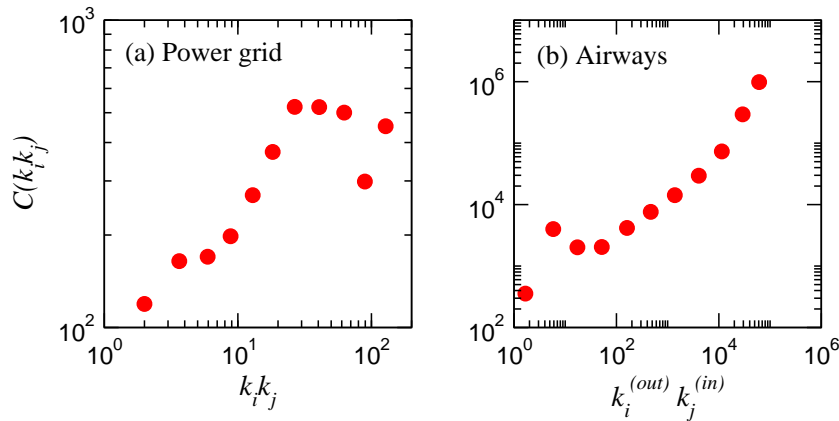


Figure A2. Capacity of the links as a function of their end-node degrees k_i and k_j in (a) the power-grid and (b) airway network. The capacity is averaged in the logarithmic scale of the degrees. Note that in (a) out-degrees and in-degrees ($k^{(out)}$ and $k^{(in)}$) are not distinguished since electric power can be transferred in both directions on the same power transmission line.

the correlation between the empirical load and the betweenness centrality is not meaningfully strong. The Pearson correlation coefficient between the two quantities is 0.27 for the power-grid network and 0.02 for the airway network. This weak correlation indicates that transport in real networks is a process considerably different from that suggested by betweenness centrality.

Figure A2 shows the relationship between the degree, another widely used graph-theoretical centrality, and the empirical capacity in the power-grid and airway network. In the airway network, the behavior of the capacity is comparable with $\sim (k_i^{(out)} k_j^{(in)})^\theta$ found in previous studies [35]. The power-grid network exhibits a stronger deviation from this power-law behavior, particularly for links with large $k_i k_j$'s. Therefore, the distribution of traffic loads and capacities in real networks is indeed more complex than expected from graph-theoretic centralities, such as betweenness centrality and degrees.

Appendix B. Superlinear cost functions

Generalizing our analysis to nonlinear cost functions [59], we can write the objective function as

$$F = (1 - w)\xi(C) + w \left(\frac{C}{C_{\max}} \right)^\nu, \quad (\text{B.1})$$

and examine how the overloading probability ξ depends on ν . Here we consider the case of superlinear functions ($\nu > 1$) in the uncorrelated fluctuation regime.

In this case, $dF/dC = 0$ leads to

$$\frac{C - L}{gL^{1/2}} = \sqrt{\log \left(\frac{1}{g\sqrt{\pi}} \frac{1 - w}{w} \frac{1}{L^{1/2}} \frac{C_{\max}^\nu}{\nu C^{\nu-1}} \right)}, \quad (\text{B.2})$$

which indicates that $(C - L)/L^{1/2}$ is a decreasing function of L . The decreasing behavior of $(C - L)/L^{1/2}$ is clear for an increasing function $C(L)$ because the right hand side of (B.2) decreases when both C and L increase. If $C(L)$ is a decreasing function, the term $(C - L)/L^{1/2}$ itself becomes a decreasing function of L . The monotonically increasing behavior of $C(L)$ is generally valid for $C \gg L$. When $C(L)$ approaches $C = L$, where the overloading probability is almost saturated, the cost function can dominate the objective function. If that is the case, the minimization of F is achieved by decreasing C even if L increases. This only happens when L is very large and can be regarded as an artifact of our selection of the cost functions. The overloading probability ξ can be written explicitly using the error function $\text{erf}(x)$ as

$$\xi = \frac{1}{2} \left[1 - \text{erf} \left(\frac{C - L}{gL^{1/2}} \right) \right]. \quad (\text{B.3})$$

Since we have shown that $(C - L)/L^{1/2}$ is a decreasing function of L , using the fact that $\text{erf}(x)$ is an increasing function of x , it is straightforward to show that the overloading probability ξ is an increasing function of the load L . The behavior of $\xi(L)$ is thus similar or more pronounced than for the linear case $\nu = 1$, indicating that the main results remain valid for $\nu > 1$.

References

- [1] Gellings C W and Yeager K E 2004 *Phys. Today* **57** 45–51
- [2] Harman B A and Lukose R M 1997 *Science* **277** 535–7
- [3] Daganzo C F 1997 *Fundamentals of Transportation and Traffic Operations* (Oxford: Elsevier)
- [4] Odlyzko A M 2003 *Review of Network Economics* **2** 210–237
- [5] Newman M E J, Barabási A-L and Watts D J (eds) 2006 *The Structure and Dynamics of Networks* (Princeton: Princeton University Press)
- [6] Dorogovtsev S N, Goltsev A V and Mendes J F F 2007 *Preprint* arXiv:0705.0010v6 [cond-mat.stat-mech]
- [7] Albert R, Jeong H and Barabási A-L 2000 *Nature* **406** 378–82
- [8] Callaway D S, Newman M E J, Strogatz S H and Watts D J 2000 *Phys. Rev. Lett.* **85** 5468–71
- [9] Cohen R, Erez K, ben-Avraham D and Havlin S 2000 *Phys. Rev. Lett.* **85** 4626–9
- [10] Cohen R, Erez K, ben-Avraham D and Havlin S 2001 *Phys. Rev. Lett.* **86** 3682–5

- [11] Shargel B, Sayama H, Epstein I R and Bar-Yam Y 2003 *Phys. Rev. Lett.* **90** 068701
- [12] Solé R V, Rosas-Casals M, Corominas-Murtra B and Valverde S 2008 *Phys. Rev. E* **77** 026102
- [13] Arenas A, Díaz-Guilera A and Guimerà R 2001 *Phys. Rev. Lett.* **86** 3196–9
- [14] Holme P 2003 *Adv. Complex Syst.* **6** 163–76
- [15] Toroczkai Z and Bassler K E 2004 *Nature* **428** 716
- [16] Noh J D, Shim G M and Lee H 2005 *Phys. Rev. Lett.* **94** 198701
- [17] Sreenivasan S, Cohen R, López E, Toroczkai Z and Stanley H E 2007 *Phys. Rev. E* **75** 036105
- [18] Watts D J 2002 *Proc. Natl. Acad. Sci. USA* **99** 5766–71
- [19] Motter A E and Lai Y-C 2002 *Phys. Rev. E* **66** 065102(R)
- [20] Holme P and Kim B J 2002 *Phys. Rev. E* **65** 066109
- [21] Moreno Y, Pastor-Satorras R, Vázquez A and Vespignani A 2003 *Europhys. Lett.* **62** 292–8
- [22] Crucitti P, Latora V and Marchiori M 2004 *Phys. Rev. E* **69** 045104(R)
- [23] Albert R, Albert I and Nakarado G L 2004 *Phys. Rev. E* **69** 025103(R)
- [24] Kinney R, Crucitti P, Albert R and Latora V 2005 *Eur. Phys. J. B* **46** 101–7
- [25] Zhao L, Park K H, Lai Y-C and Ye N 2005 *Phys. Rev. E* **72** 025104
- [26] Lee E J, Goh K-I, Kahng B and Kim D 2005 *Phys. Rev. E* **71** 056108
- [27] Kim D-H, Kim B J and Jeong H 2005 *Phys. Rev. Lett.* **94** 025501
- [28] Motter A E 2004 *Phys. Rev. Lett.* **93** 098701
- [29] Gallos L K, Cohen R, Argyrkis R, Bunde A and Havlin S 2005 *Phys. Rev. Lett.* **94** 188701
- [30] Schäfer M, Scholz J and Greiner M 2006 *Phys. Rev. Lett.* **96** 108701
- [31] Zhao X M and Gao Z Y 2007 *Eur. Phys. J. B* **59** 85-92
- [32] Wang B and Kim B J 2007 *Europhys. Lett.* **78** 48001
- [33] Li P, Wang B-H, Sun H, Gao P and Zhou T 2008 *Eur. Phys. J. B* **62**, 101–4.
- [34] Buzna L, Peters K, Ammoser H, Kuhnert C and Helbing D. 2007 *Phys. Rev. E* **75** 056107
- [35] Barrat A, Barthélemy M, Pastor-Satorras R and Vespignani A 2004 *Proc. Natl. Acad. Sci. USA* **101** 3747–52
- [36] Guimerà R, Mossa S, Turttschi A and Amaral L A N 2005 *Proc. Natl. Acad. Sci. USA* **102** 7794–9
- [37] Yook S H, Jeong H, Barabási A-L and Tu Y 2001 *Phys. Rev. Lett.* **86** 5835–8
- [38] Barrat A, Barthélemy M and Vespignani A 2004 *Phys. Rev. Lett.* **92** 228701
- [39] Carreras B A, Newman D E, Dobson I and Poole A B 2004 *IEEE Trans Circuits Syst I: Fundam Theory Appl* **51** 1733–40
- [40] Dobson I, Carreras B A, Lynch V E and Newman D E 2007 *Chaos* **17** 026103
- [41] Jensen H J 1998 *Self-Organized Criticality* (Cambridge: Cambridge University Press)
- [42] Air Transport Consultancy Services 2003 *Airport Capacity/Demand Profiles* (Geneva: International Air Transport Association)
- [43] Transportation Research Board 2002 *Highway Capacity Manual* (Washington, DC: Transportation Research Board)
- [44] Youn H, Gastner M T and Jeong H 2007 *Preprint* arXiv:0712.1598v2 [physics.soc-ph]
- [45] Guclu H, Korniss G and Toroczkai Z 2007 *Chaos* **17**, 026104
- [46] Arollo de Menezes M and Barabási A-L 2004 *Phys. Rev. Lett.* **92** 028701
- [47] Arollo de Menezes M and Barabási A-L 2004 *Phys. Rev. Lett.* **93** 068701
- [48] Duch J and Arenas A 2006 *Phys. Rev. Lett.* **96** 218702
- [49] Kim D-H and Motter A E 2008 *J. Phys. A: Math. Theor.* in press (*Preprint* 0801.1877v1 [physics.soc-ph])
- [50] Karagiannis T, Molle M and Faloutsos M 2004 *IEEE Internet Computing* **8** 57–64
- [51] Gnedenko B V and Kolmogorov A N 1954 *Limit Distributions For Sums of Independent Random Variables* (Cambridge: Addison-Wesley)
- [52] Gumbel E J 1958 *Statistics of Extremes* (New York: Columbia University Press)
- [53] Li L, Alderson D, Willinger W and Doyle J 2004 *Proc. SIGCOMM'04 (Portland, Oregon, USA)* p 3–14 (<http://doi.acm.org/10.1145/1015467.1015470>)
- [54] McCarthy P S and MaCarthy T 2001 *Transportation Economics: Theory and Practice* (Malden:

BlackWell)

- [55] Freeman M L 1977 *Sociometry* **40** 35–41
- [56] Newman M E J 2001 *Phys. Rev. E* **64** 016132
- [57] Goh K-I, Oh E, Jeong H, Kahng B and Kim D 2002 *Proc. Natl. Acad. Sci. USA* **99** 12583–8
- [58] Kim D-H, Noh J D and Jeong H 2004 *Phys. Rev. E* **70** 046126
- [59] Aldous D J 2008 *J. Stat. Mech.* P03006